CHARACTERIZATION OF THE DENDRITIC MICROSTRUCTURE OF INVESTMENT CAST ALLOY 718

Y.K. Ko and J.T. Berry

Department of Metallurgical and
Materials Engineering
University of Alabama
Tuscaloosa, AL 35487-0202
P.O. Box 870202

Abstract

The as-cast alloy 718 shows a multiphasic structure which consists of dendrites, carbides and Laves phases. The amount, size, shape, and dispersion of these phases affect the properties and the processing which follows. This structure was characterized by measurements of volume fraction, size, dispersion, and shape factor of carbide and Laves phases. Secondary arm spacing and Vickers hardness were also measured in the as-cast condition. All the above measurements were carried out on two different sized castings which had different cooling conditions. Compositional analysis of the phases in the castings concerned are clearly linked to solidification behavior of the alloy. These values were statistically analyzed to distinguish the effects of the casting conditions.

Superalloys 718, 625, 706 and Various Derivatives
Edited by E.A. Loria
The Minerals, Metals & Materials Society, 1994

Introduction

Superalloy 718 is one of the most heavily utilized nickel-iron base structural materials. It has high strength, corrosion and oxidation resistance, and good creep and fatigue resistance at moderately elevated temperatures.[1] The nominal composition of the alloy in weight percent is 18Cr, 18Fe, 5Nb, 3Mo, 1Ti, 0.5Al, 0.04C, and 0.004B.[2]

The alloy experiences the precipitation of a number of important phases during freezing. These include, for example MC carbides at temperatures at or above the solidus. Since diffusion rates in the solid state are generally slow, certain aspects of the microstructure of the alloy will be virtually fixed after solidification. Thus, the solidification determines distribution and size of carbide particles. Shape and location of the carbides are also affected by the solidification process. These characteristics of the carbides contribute to the mechanical properties of the alloy at room temperature and/or at elevated temperature. The Laves phase is also present in this alloy and constitutes a microstructural weakness which promotes decohesion under a tensile stress, since it melts at a lower temperature than the matrix. This Nb-rich phase also depletes the potential for gamma double prime precipitate strengthening. The phase usually undergoes decomposition and its constituents are diffused into matrix during the homogenization process. The initial size and dispersion of the Laves thus clearly affect the success of the homogenization process. Additionally, pronounced segregation and dispersed porosity formation are sometimes experienced during the solidification process.[3]

Ideally, it would be desirable to be able to predict the life potential of each critical superalloy component prior to its use.[4] The life of such components is clearly affected by their microstructure. In this respect the characterization of the microstructure observed in this alloy becomes extremely important. In the present investigation, microstructural features such as secondary arm spacing, carbide size, shape factor and its dispersion, Laves shape factor and cluster dispersion were measured in two castings which represent extremes in casting conditions. Vickers hardness and local chemical composition were also measured. The values obtained were statistically tested in order to determine the extent of the effects of the two different casting conditions.

Experimental Procedures

Cast samples of 718 alloy were supplied by a commercial investment caster. The composition of the alloy was given in weight percent as 53.4Ni, 18.95Fe, 18.01Cr, 4.94Nb, 2.95Mo, 0.86Ti, 0.53Al, 0.09Si, and 0.056C. The pouring conditions of the various cast bars are shown in Table 1. Prior to pouring thermocouples were installed in central location within the mold cavities to obtain cooling curve data. The section sizes cast were from 9 to 38 mm in diameter, and were cylindrical in shape.

Sample Preparation

The bars concerned were sectioned across a central diametral plane below the thermocouple sites. Samples were polished and carbon coated for compositional analysis, or electro-etched for morphological analyses. The etching solution used was 5% oxalic acid.

Microstructural Characterization

Microstructural characterization was carried out using an Olympus C-2 Vision Image Analysis System and a JEOL 8600 Electron Microprobe Analyzer. The characterization included the measurement of phase volume fraction, size distribution, dispersion, secondary dendrite arm spacing, as well as compositional analysis of individual phases. The various characterizations were performed principally at the two extreme casting conditions, which were represented by low cooling rate (No.15 large casting) and high cooling rate (No.14 small casting) conditions.

Results and Discussion

The as-cast material shows a composite type microstructure which consists of Laves and carbide particles distributed within a dendritic microstructure, as shown in Figure 1. Carbide particles appear within the dendrites, as well as in the interdendritic regions. The Laves phases occur exclusively in the latter. Shrinkage cavities were also present in the centers of the two subject castings.

Table I Pouring Conditions in IN 718

Casting	Condition	Dim.(mm) D	Dim.(mm) L	Mold Temp.	Pouring Temp.	After Casting
No. 14 Casting	Large	38	180	1500°F	2800°F	Blowing Air
	Medium	19	180	〃	〃	〃
	Small	9	180	〃	〃	〃
No. 15 Casting	Large	38	180	2800°F	2800°F	Under Vacuum
	Medium	19	180	〃	〃	〃
	Small	9	180	〃	〃	〃

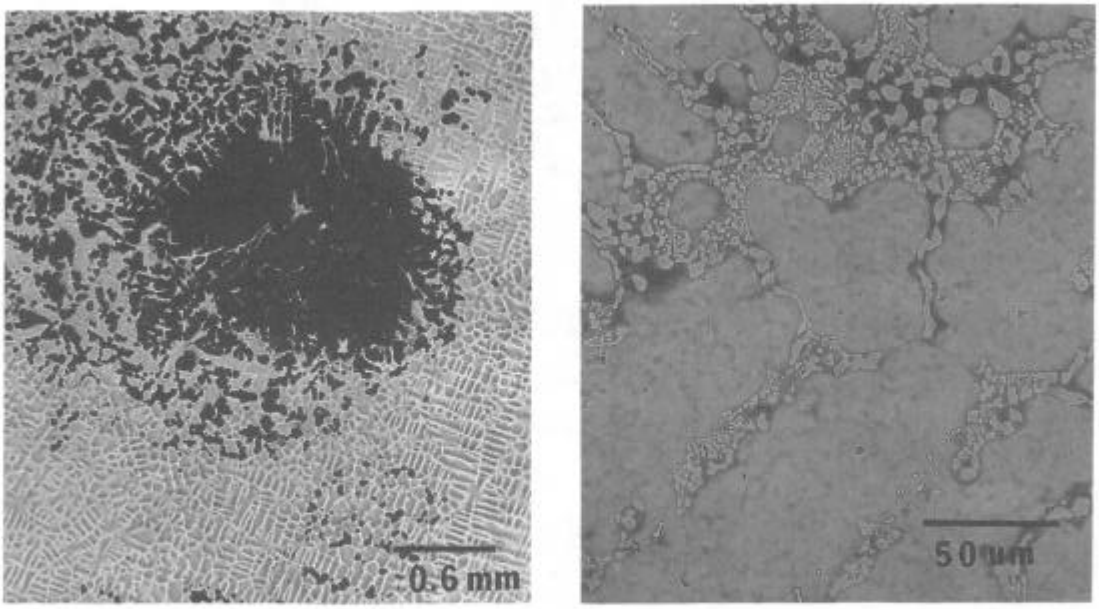

Figure 1 - Microstructures of IN 718 castings showing shrinkage cavities (left) and composite type structure (right) at the centers of small and medium sized castings respectively.

Secondary Arm Spacing

Figure 2 shows secondary arm spacing measurements in three of the castings. Variation of secondary arm spacing in the small casting is much less than that in the large casting. The values of the secondary arm spacing are smaller and are almost same near the casting surface and at the center in the small casting. This indicates that the dendritic growth rate is more uniform and solidification time does not vary greatly throughout this cross-section. This would imply that the smaller casting should possess a more uniform chemical composition than the larger one. The smaller secondary arm spacing in the small casting clearly establishes that solidification time was less than that of the large casting. The finer scale microstructure would be expected to exhibit superior mechanical properties.

The values of secondary arm spacing at the center of the bigger casting are large in comparison with the above and show considerable variation. This implies a longer solidification time, and further that significant segregation is likely to have occurred. Irregular temperature gradients, uneven growth rates and segregation patterns could probably have been experienced in the central region of this casting because of the significant shrinkage formation. One, or more of these effects probably contributed to the large variation of the secondary arm spacing.

The fine scale microstructures observed in the smaller casting are noteworthy. Such features would be associated with small interdiffusion distances. Consequently, niobium within the Laves phase would be easily redistributed during the homogenization process. This would lead to uniform distribution of gamma double prime/gamma prime phases during heat treatment and thus provide for improved mechanical properties. Porosity, which is often associated with the presence of Laves, will be also reduced by increasing solidification rate, since this provides less segregation and less time for nucleation. The absence of this porosity also assists in obtaining the superior mechanical properties associated with finer microstructures.

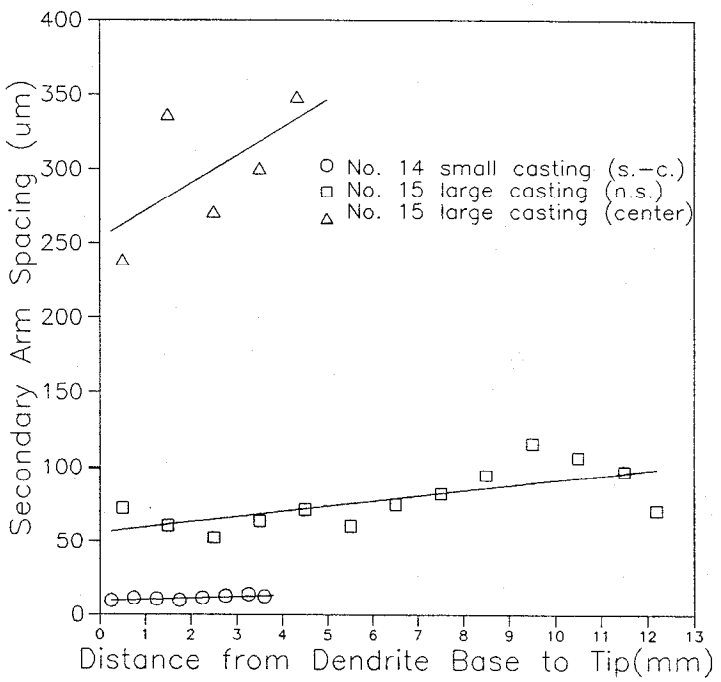

Figure 2 – Secondary arm spacing of IN 718 castings measured from dendrite base to tip.

Carbide Size Distribution and Carbide Dispersion

Carbide size distribution in the small, medium and large castings is summarized in Table 2. In the interdendritic regions, the average carbide size is larger than that associated with the dendritic region. This difference probably results from the segregation of carbon and niobium to interdendritic regions and longer contact time with the melt in this region. If one assumes a given volume fraction of carbide for all castings concerned, the overall mean spacing probably increases as the particle size increases. This will occur since the number of particles must

Table II Mean Spacing and Average Size of Carbide in IN 718 Casting

Casting Position	Carbide Location	Mean Carbide Spacing, σ (mm)	Average Size of Carbide (μm)	Standard Deviation
No. 14 Small Near Sur.	Dendrite	0.210	2.03	0.85
	Interdendrite	0.139	2.68	1.29
	Overall Avg.	0.176	2.30	1.10
No. 14 Medium Near Sur.	Dendrite	0.372	2.83	1.17
	Interdendrite	0.152	3.76	1.30
	Overall Avg.	0.278	3.18	1.30
Inter.	Dendrite	0.510	2.34	0.96
	Interdendrite	0.106	3.79	1.58
	Overall Avg.	0.301	2.93	1.44
Center	Dendrite	0.397	2.93	1.14
	Interdendrite	0.115	4.14	1.52
	Overall Avg.	0.248	3.48	1.45
No. 15 Large Center	Dendrite	2.571	6.58	2.38
	Interdendrite	0.122	8.26	6.36
	Overall Avg.	0.284	8.14	6.18

decrease as the particle size increases for a given carbon content. Overall measurements shown in Table 2 match this trend. However, the average mean carbide spacings at the center of the medium size casting and at the center of the large casting do not match the above pattern. The regions in which these carbides are located, however, are probably associated with segregation of carbide forming elements (Nb, Ti, C, etc.) and also with a longer contact time with the melt. Massive Laves phase due to Nb segregation were also found within interdendritic regions in center of medium size casting, as shown in Figure 1. The mean carbide spacing in these interdendritic regions is smaller in comparison with that in the corresponding dendritic regions.

Figure 3 compares carbide size distributions in corresponding dendritic regions and interdendritic regions in the small casting. The average carbide sizes in interdendritic regions are greater than these in the dendritic regions. These data show that wide carbide distribution ranges are associated with interdendritic regions. Figure 4 shows that a large number of carbides were segregated to the interdendritic region in the center of the large casting and that large and elongated carbides were formed in this region. From Table 2 and Figure 5 it will be seen that the carbide forming elements in the intermediate regions or mid-radius locations in the medium size casting were probably segregated to central region as a result of the competitive growth among the columnar dendrites. The value of mean carbide spacing is larger and the average size of carbide smaller within dendrites in the intermediate region than in the two other regions. Carbide size distributions in this intermediate region are narrow, as shown in Figure 5. This probably indicates that solidification rates were similar throughout such a region. Figure 6 shows the ranges of carbide size distribution and their average sizes. From this figure it will also be seen that the small casting exhibits a more uniform size distribution of carbide, and probably a lower degree of segregation of carbide forming elements, than that seen in the larger casting.

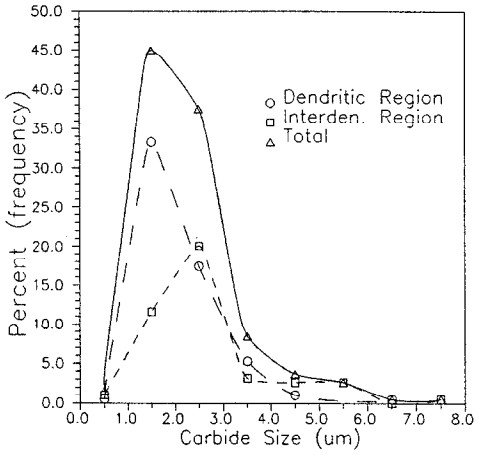

Figure 3 - Size distribution of carbides at near surface in the small casting.

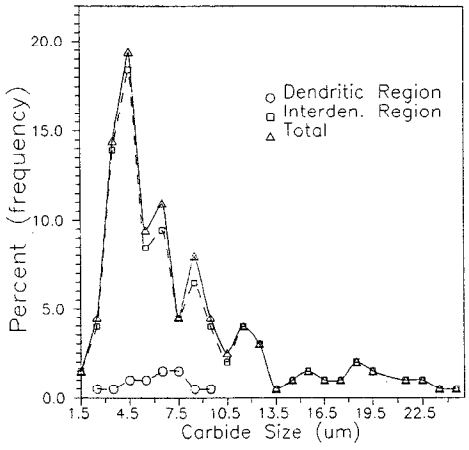

Figure 4 - Size distribution of carbides at the center in the large casting.

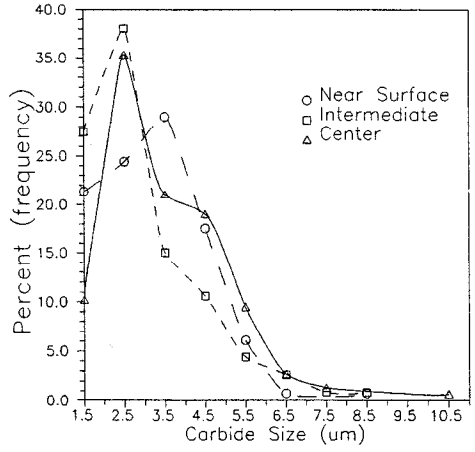

Figure 5 - Size distribution of carbides in the medium sized casting.

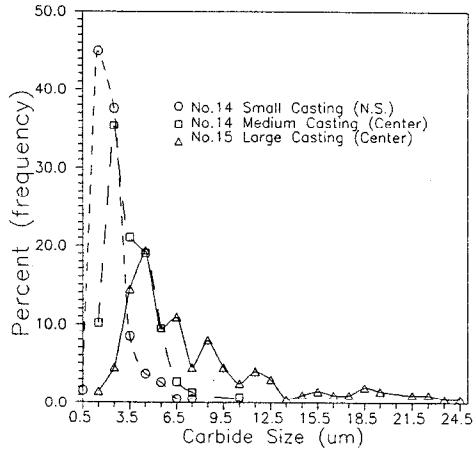

Figure 6 - Size distribution of carbides in the three different sized casting.

Dispersion of carbide particles was next examined. This can be quantified by measuring the minimum interparticle distance.[5] These measurements of the minimum interparticle distance show lower values than the mean spacing in Table 2. Figure 7 shows a good dispersion of carbide at near surface locations in the small casting. Carbide dispersion in the large casting shows two peaks, one of which was associated with the smaller interparticle distance through the interdendritic region, while the other, a larger interparticle distance was exhibited across the dendrite at the center of the large casting. This once again indicates that the carbides tend to be segregated to the interdendritic regions. Furthermore, this figure shows that the small casting possesses a much more uniform dispersion of carbides than the large casting. This would be expected to lead to superior mechanical properties in the small casting.

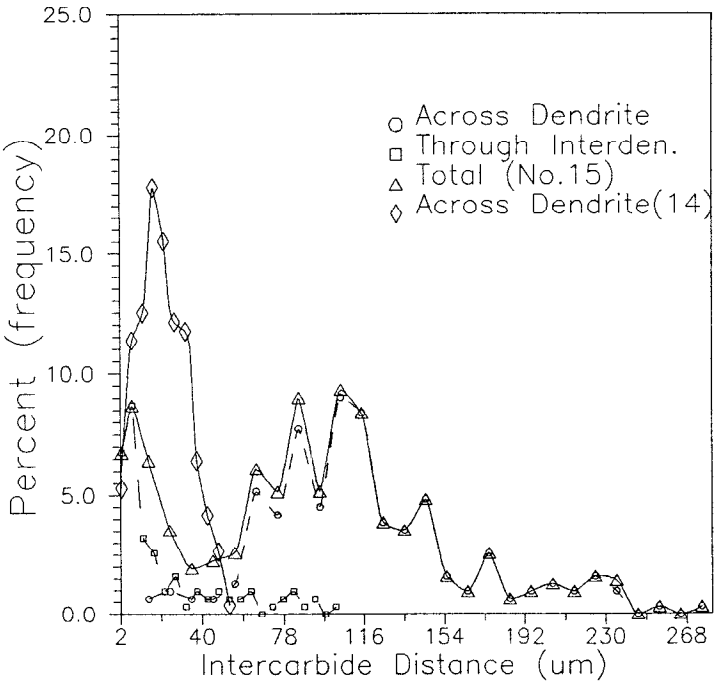

Figure 7 – Dispersion of carbides at the center of cross-section in the middle of IN 718 large casting (No.15, lower cooling rate) and at near surface of the small casting (No.14).

Laves Cluster Dispersion

Figure 8 show the dispersion of Laves clusters in the small casting and in the large casting. The Laves clusters in the small casting were usually isolated by dendrites and the intercluster distances were measured across individual dendrites. However, it will be seen that the dispersion of Laves clusters in the large casting shows two peaks. These peaks reflect lower values measured through the interdendritic region and higher values measured across dendrites itself. These irregularities indicate that the Laves clusters were mainly segregated to the interdendritic region. The interdendritic regions containing Laves clusters are usually inter-connected in the large casting. Therefore, mechanical properties would again be expected to be inferior in the large casting. The inter-connected interdendritic region and Laves phase would also possess lower local melting ranges than the dendrite cores. However, the small casting possesses a smaller intercluster distances and a more uniform distribution of Laves clusters than the large casting. These factors again would seem to be an indication of superior and reproducible mechanical properties.

Volume Fraction and Compositional Analysis of Phases

Volume fractions were calculated by the systematic manual point count method described in ASTM E 562. The volume fractions of carbide and Laves are shown in Table 3. Standard deviations of the volume fraction are high and the volume fractions of carbide and Laves in the large casting do not compare well with those of the small casting. However, the point count method probably shows higher values for large numbers of small objects present in low volume fractions than for larger objects.

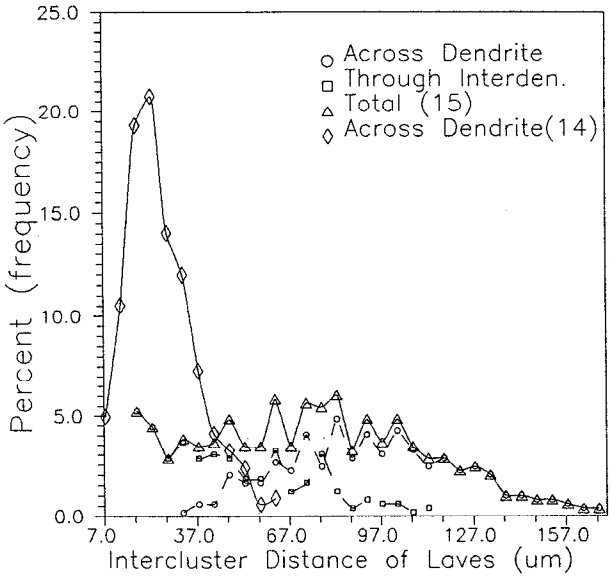

Figure 8 – Dispersion of Laves clusters at the center of cross-section in the middle of IN 718 large casting (No.15, lower cooling rate) and at near surface of the small casting (No.14)

Compositions of the various phases are shown in Table 4. This compositional analysis shows that Nb, Mo, Ti, and Si were rejected during dendritic growth. These elements exhibit a minimum concentration at the dendrite cores and an increased concentration within the interdendritic regions. Conversely, Fe, Ni, and Cr concentration decreased from the dendrite core into the interdendritic region. A mixed image of secondary and backscattered electrons at center of the small casting in Figure 1 shows the segregation of the heavy elements, as shown in Figure 9. In the small casting, the average concentrations of Ni and Cr are lower within dendrites than those in the large casting. This suggests that Ni and Cr atoms were more concentrated to the primary solid than Fe during the solidification of the large casting. The summation of the three major element concentrations of matrix (Fe, Ni, and Cr) shows that the large casting has higher values within the dendrites than has the small casting. This indicates, once again, that segregation is more serious in the large casting.

Table III Volume Fraction of Phases

Casting Position	Phase	Total No. of Count	Average No. of Count	Standard Deviation	Volume Fraction (%)
No. 14	Car.& Laves	65	3.25	1.902	5.159
Small	Carbide	21.5	1.08	0.712	1.706
Near Sur.	Laves				3.453
No. 14	Car.& Laves	63.5	3.18	1.340	5.040
Medium	Carbide	12	0.6	0.553	0.952
Near Sur.	Laves				4.088
	Car.& Laves	60	3	1.112	4.762
Inter.	Carbide	11.5	0.58	0.712	0.913
	Laves				3.849
	Car.& Laves	63.5	3.18	1.727	5.040
Center	Carbide	14.5	0.73	0.617	1.151
	Laves				3.889
No. 15	Car.& Laves	57	2.85	1.434	4.524
Large	Carbide	20.5	1.03	0.575	1.627
Center	Laves				2.897

Table IV Phase Composition Data (Wt.%) of IN 718

Casting & Position	Location Dendrite	Major Ele. of Matrix Fe	Ni	Cr	Sum.	Nb	Mo	Ti	Si
No. 14	Core	21.03	53.11	19.21	93.35	2.60	2.50	0.42	0.51
Small	Intermediate	20.96	52.79	19.25	93.00	2.84	2.51	0.44	0.54
Near sur.	Near Laves	17.79	52.11	18.51	88.41	4.50	2.73	0.58	0.71
No. 15	Core	20.42	54.32	19.78	94.52	1.92	2.42	0.49	0.12
Large	Intermediate	20.15	53.79	19.61	93.55	2.18	2.47	0.54	0.14
Center	Near Interm.	19.31	52.86	19.19	91.36	4.07	2.75	0.78	0.17
	Interdendrite	16.51	52.79	18.21		6.30	3.08	1.12	0.20
	Phase								
NO. 15	Eutectic Laves	7.62	49.48	9.09		25.70	3.94	1.60	0.51
Large	Globular Laves	11.37	39.58	12.31		29.04	4.74	0.82	1.10
Center	MC Carbide	0.55	1.67	0.73		74.91	0.00	8.57	0.03
NO. 14	Eutectic Laves	11.99	43.81	11.34		24.88	3.40	0.77	2.88
Small	Globular Laves	11.00	40.64	10.32		29.86	4.32	0.64	3.21
Near Sur.	MC Carbide	1.14	2.72	1.45		75.51	0.00	5.09	0.03

As would be expected, Laves phases are enriched in Nb, Mo, and Si and depleted of Fe, Ni, and Cr. Nb and Si are likely to have strong effects on the propensity for Laves formation. The MC carbide is enriched in Nb and Ti and depleted of other elements. Mo does not appear to participate in the formation of MC carbides in this alloy.

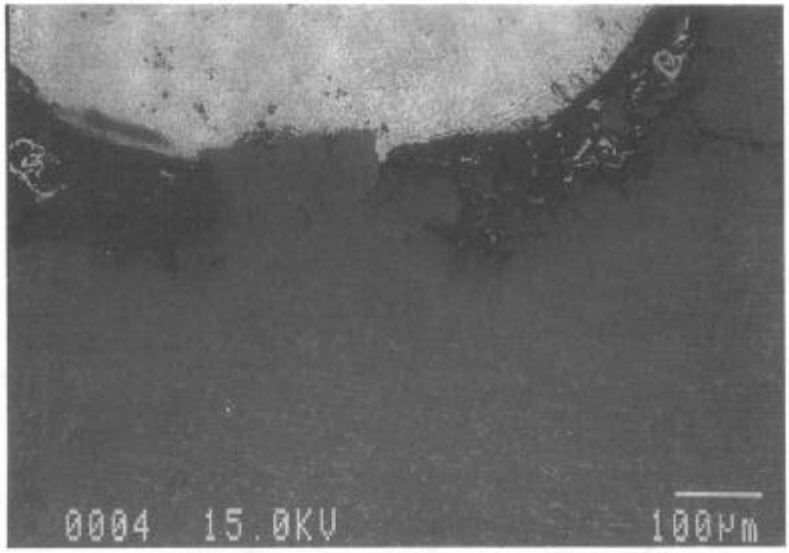

Figure 9 - A mixed image of secondary and backscattered electron at the center of the small casting in Figure 1.

Hypothesis Testing

Hypothesis testing[6] has been performed in order to evaluate qualitatively the extent to which the above measured values are statistically different. First, the difference in variances is tested. It is well known that the sample variance is distributed as chi-square (χ^2) and that the ratio of the two independent χ^2 random variables follows the F distribution. The F test was applied to distinguish the difference of the variances. Difference in mean values is also tested. An appropriate t test statistic for comparing two treatment means can be chosen depending upon the previous tests for different variances. A two-stage nested design[6] is employed to examine a compositional variation. It is applied to the data associated with core and intermediate regions within the dendrites. The zone between the cores of the dendrites and where it borders the

interdendritic region has been termed the intermediate region. All of the tests were conducted at the five-percent significance level (α=0.05).

Table V Hypothesis Testing of Dendrite Arm Spacing and Hardness

	Casting Size	n	Avg.	SD	F_o	t_o	ν
Secondary Arm Spacing	Large	13	299.914	50.683	446.34 *	20.51*	12
	Small	59	11.523	2.399			
Vickers Hardness Number	Large	30	188.860	13.181	2.47*	17.72*	51
	Small	30	239.414	8.394			

Table 5 presents the results from the F and t tests for the secondary arm spacing and the Vickers hardness number of dendrites. The results indicate that both secondary arm spacing and Vickers hardness number have different variances and different mean values in the small and large castings. The ratio of sample variances (F_o) was very large for secondary arm spacing. The reason for the ratio of variance in secondary arm spacing showing high values at center of large casting is probably due to shrinkage formation.

Table VI Hypothesis Testing for Carbide and Laves Phase

		Casting Size	Location	n	Avg.	SD	F_o	t_o	ν
Carbide	Size (μm)	Small	Interden.	79	2.681	1.290			
		Small	Dendrite	110	2.035	0.847	2.32*	3.89*	126
		Large	Interden.	187	8.258	6.315			
		Large	Dendrite	14	6.576	2.379	7.05*	2.14*	33
		Large	Interden.	201	8.141	6.183			
			+				16.02*	13.16*	214
		Small	Dendrite	189	2.305	1.100			
	Shape Factor	Small	Interden.	62	0.600	0.129			
		Small	Dendrite	93	0.685	0.127	1.03	4.04*	153
		Large	Interden.	209	0.557	0.194			
		Large	Dendrite	54	0.738	0.091	4.54*	9.91*	189
		Large	Interden.	209	0.557	0.194			
		Small	Interden.	62	0.600	0.129	2.26*	2.03*	153
		Large	Dendrite	54	0.738	0.091			
		Small	Dendrite	93	0.685	0.127	1.95*	2.93*	141
		Large	Interden.	263	0.594	0.192			
			+				2.05*	3.56*	407
		Small	Dendrite	155	0.651	0.134			
	Dis-persion (μm)	Large	Interden.	310	86.276	60.246			
			+				27.04*	18.44*	336
		Small	Dendrite	266	21.823	11.585			
Laves	Shape Factor	Large	Interden.	354	0.537	0.207			
							1.14*	0.53	416
		Small	Interden.	209	0.547	0.221			
	Dis-persion (μm)	Large	Interden.	495	76.175	38.162			
			+				11.49*	27.86*	613
		Small	Dendrite	342	25.466	11.259			

* : Rejection of H_o at α=0.05

Table 6 reports the results using the carbide and Laves phase data. The variance ratio computed from the carbide sizes in the small casting is smaller than that in the large casting.

This again indicates that small casting contains a more uniform size of carbides than the large casting. Furthermore, all of the variances and mean values in the size categories are different at α=0.05. This indicates that the casting conditions do affect the carbide sizes and the size distributions. The variance ratio computed from the carbide shape factor compares the lowest value in small casting and the highest value in large casting. The results indicate that the variances of carbide shape factor in small casting are similar, but are different from those in the large casting. Tests for different mean values using shape factors show that these are different depending on the casting sizes and locations in the castings. In particular, the large casting resulted in large values of the test statistics. Therefore, the large casting contains quite different shapes of carbides in dendritic and interdendritic region.

The variance ratio of Laves shape factor shows differences in the small and large castings. The test statistic (t_o) for mean values, however, does not show a significant difference between each casting. This indicates that the overall shape of Laves phase is similar in both castings. This further suggests that the casting conditions are not significant factors determining the Laves shape.

The interparticle distances of carbide and the intercluster distances of Laves show different variances and different means in both castings. The casting conditions thus affect these distances, especially, the carbide dispersion.

Table VII Hypothesis Testing of Alloying Elements

	Casting Size	Location	Avg.	SD	F_o Location	F_o Casting	t_o Casting	ν
Fe	Large	Core	20.42	0.215	0.45	11.62*	3.52*	17
		Interme.	20.15	0.433				
	Small	Core	21.03	0.623				
		Interme.	20.96	0.493				
Ni	Large	Core	54.32	0.292	1.87	23.81*	4.64*	18
		Interme.	53.79	0.428				
	Small	Core	53.11	0.490				
		Interme.	52.79	0.719				
Cr	Large	Core	19.78	0.213	1.28	33.01*	5.74*	19
		Interme.	19.61	0.154				
	Small	Core	19.21	0.181				
		Interme.	19.25	0.168				
Nb	Large	Core	1.92	0.046	1.61	22.40*	4.61*	12
		Interme.	2.18	0.109				
	Small	Core	2.60	0.363				
		Interme.	2.84	0.500				
Mo	Large	Core	2.42	0.050	0.54	2.83	1.52	18
		Interme.	2.47	0.026				
	Small	Core	2.50	0.108				
		Interme.	2.51	0.091				
Ti	Large	Core	0.49	0.019	3.16	30.04*	5.10*	18
		Interme.	0.54	0.022				
	Small	Core	0.42	0.045				
		Interme.	0.44	0.046				
Si	Large	Core	0.12	0.004	1.52	1026.77*	31.50*	12
		Interme.	0.14	0.013				
	Small	Core	0.51	0.035				
		Interme.	0.54	0.041				

* : Rejection of H_o at α=0.05

Table 7 shows the test results for local chemical compositions at core and intermediate regions in the various dendrites. The variance ratios at locations within the core and the intermediate

regions within the dendrites do not show significant differences for a given casting. This indicates that all the elements are not significantly segregated in these regions for the same casting condition. However, the ratios of variances based on the two castings show significant differences for all elements examined except for molybdenum. This implies that all the elements except for Mo, are significantly affected by the casting condition. Test for different mean values also indicates that all elements have different values except for molybdenum. Consequently, Mo is the least affected element by the two different casting conditions. On the other hand, the rejection of the same means and variances was the strongest for Si, suggests that it is the most affected elements.

Conclusions

Hypothesis testing provides numerical values which allow one to compare effects upon microstructure with each other qualitatively. From the hypothesis testing, the following conclusions were deduced.

1. All microstructural features measured were affected by the casting conditions except Laves shape factor.

2. Within a given casting, none of the chemical elements were significantly segregated at core and intermediate regions of the dendritic microstructures observed, whereas all the elements except molybdenum were segregated according to the different casting conditions.

3. Molybdenum is the least affected element and Si is the most affected element in terms of the casting condition.

Acknowledgements

The authors wish to acknowledge Dr. R.A. Overfelt (Auburn university, subcontract monitor) and NASA for the provision of support throughout this investigation. Dr. M.G. Bersch (U.A) and Dr. M.J. Kim (U.A) must be thanked for valuable discussions. Dr. K.O. Yu (CTC) and Mr. M. Robinson (Robinson Products) must also be acknowledged for the supply of materials.

References

1. G.A. Knorovsky et al., "INCONEL 718: A Solidification Diagram," Metallurgical Trans., Vol.20A, (1989), 2149-2158.

2. J.F. Radavich, "The Physical Metallurgy of Cast and Wrought Alloy 718," Superalloy 718-Metallurgy and Applications, (1989), 229-240.

3. A. Mitchell, "Melting Processes and Solidification in Alloys 718-625," Superalloys 718, 625 and Various Derivatives, (1991), 15-27.

4. C. Peyroutou and Y. Honnorat, "Characterization of Alloy 718 Microstructures," Superalloys 718, 625 and Various Derivatives, (1991), 309-324.

5. F. Rana, "SiC Particle Dispersion in Aluminum Alloy Metal-Matrix Composites," M.S. Thesis, University of Alabama., May 1989.

6. D.C. Montgomery, Design & and Analysis of Experiments (John Wiley & Sons, 1984), 21-38, 357-374.